PRECISION PROCESSING OF HIRISE STEREO ORBITAL IMAGES FOR TOPOGRAPIC MAPPING ON MARS

Juwon Hwangbo[1], Yunhang Chen[2], and Rongxing Li[2]
[1] Chief Photogrammetrist
M7 Visual intelligence
510 Bering Drive, Suite 310, Houston, TX 77057
juwon.hwangbo@m7vi.com
[2] Mapping and GIS Laboratory
Dept. of Civil & Environmental Engineering & Geodetic Science, The Ohio State University
470 Hitchcock Hall, 2070 Neil Avenue, Columbus, OH 43210
chen.1256@osu.edu, li.282@osu.edu

ABSTRACT

To build HiRISE image network with the best possible precision and accuracy, technical issues involving sensor geometry and absolute positioning need to be resolved. High-frequency random patterns, or "jitter", in the rotation angles cause disagreements between HiRISE CCDs. To generate seamless topographic products, it is important to achieve coherence in the exterior orientation parameters between multiple CCDs. Also, new images should be registered to the existing global geodetic control network to achieve absolute positioning in global scale. This paper focuses on bundle adjustment based on rigorous sensor modeling of HiRISE imagery and absolute positioning using MOLA control network. For construction of orbital image networks, bundle adjustment system using traditional and inter-CCD tie points is developed to resolve misalignment of exterior orientation parameters between stereo images and CCDs. The bundle adjustment method based on third-order polynomials reduced mean back projection error of traditional tie points from over 3 pixels to less than 0.2 pixel for the test dataset covering Spirit rover landing site. The back projection residual between inter-CCD tie points were also reduced to about half a pixel. For absolute geopositioning without ground-control points, HiRISE DTM is first matched with MOLA MEDGR DTM and then with PEDR profile after bundle adjustment. The absolute positioning result is compared with the Spirit rover landing position visible on the HiRISE image. The displacement is reduced from about 200 m to 65 m, which is successful given the MOLA horizontal accuracy of 100 m.

INTRODUCTION

Orbital mapping is the fundamental element in planetary exploration programs, providing global and local maps of the Martian surface that are utilized for identifying and registering the target of scientific investigation. Detailed three-dimensional (3-D) topographic information of the terrain produced from stereo photogrammetry not only gives insights about geomorphology of the planet, but also provides significant supports to planetary surface missions. Mars orbital data have been used to generate global and local topographic information for landing-site selection, precision landing, and surface operations in Mars Exploration landed missions (Li et al., 2004, 2005, 2008).

In the past a few decades, there has been great progress in the resolution of the orbiter sensors. Before the sub-meter resolution (0.25 m/pixel) imagery from High Resolution Imaging Science Experiment (HiRISE) became available, the maximum resolution achieved by orbital sensor was 1.5 m/pixel from Mars Orbiter Camera (MOC) Narrow Angle (NA) images. Majority of MOC NA images were obtained in the resolution of 3 m/pixel, which can produce high quality digital terrain models (DTMs) (10 m grid spacing). However, overlapping images suitable for stereo mapping were rare (Li et al., 2004). As of October 2009, several hundred HiRISE stereo pairs have been acquired, making meter-scale topographic mapping of Mars possible for locations where high-resolution stereo images were not available previously. To achieve the full potential of such advanced sensor and its vast coverage, it is of paramount importance to build HiRISE image network with the best possible precision and accuracy.

The unique HiRISE sensor configuration consists of 14 CCDs fixed to a focal plane. The complexity of the sensor geometry raises technical issues that need to be resolved in HiRISE stereo processing when it is used for the generation of high-resolution topographic products such as DTMs or orthophotos. High-frequency random patterns, or "jitter", in the rotation angles cause disagreements between HiRISE CCDs. To generate seamless topographic products, it is important to achieve coherence in the exterior orientation parameters between multiple CCDs.

Another issue involving construction of orbital image networks is accurate geopositioning of HiRISE data without ground-control points. Due to the Doppler shift measurements, the observed trajectories of the orbiters could be affected by systematic shifts and drifts in the magnitude of hundreds or thousands of meters. To achieve absolute positioning in global scale, new images should be registered to the existing global geodetic control network.

In this paper, a methodology for bundle adjustment of HiRISE stereo images and absolute positioning using Mars Orbiter Laser Altimeter (MOLA) control network is presented. Bundle adjustment strategies using polynomial function models are applied to improve the exterior-orientation parameters. The MOLA Mission Experiment Gridded Data Record (MEDGR) having a resolution of 463 m per pixel provides the best source of ground control. However, the big difference in planimetric resolution between the HiRISE imagery and MOLA DTM prevents achieving horizontal accuracy better than hundreds of meters when MEDGR is used as direct source of horizontal control. Kirk et al. (2008) used coordinates measured from the 1.5 m/pixel MOC images previously controlled to MOLA for horizontal control points. In this research, HiRISE DTM is matched with interpolated MOLA DTM to obtain an initial estimate of the absolute position of the stereo model.

.

PHOTOGRAMMETRIC PROCESSING OF HIRISE IMAGERY

HiRISE is a push-broom imaging sensor with 14 CCDs (10 red, 2 blue-green and 2 NIR). Each CCD consists of a block of 2048 pixels in the across-track direction and 128 pixels in the along-track direction. Ten CCDs covering the red spectrum (700 nm) are located in the middle. In the across-track direction, average overlap width between adjacent CCDs is about 48 pixels. However, the alignment of CCDs involves small shifts and rotations with regarding to the HiRISE optical axis. After excluding overlapping pixels, HiRISE can generate images with a swath of up to 20,264 pixels (across-track) and a resolution of 30 cm/pixel at an altitude of 300 km (McEwen et al, 2007). Detailed specification of the HiRISE CCD alignment and the sensor calibration results can be found in Kirk et al. (2008).

HiRISE Exterior Orientation Parameters

Exterior orientation parameters, or the positions of the camera perspective center and pointing angles at a specific time, are provided in the SPICE kernels (Acton, 1999). The exterior orientation parameters of each image line can be retrieved by interpolating the spacecraft's trajectory and pointing vectors based on the observation time. The observation time of each image line is defined as the exposure time, which can be calculated by the starting time (the exposure time of the first line) of the CCD and the line rate (the speed of line movement). Since Each CCD is operated separately, the starting time differs from CCD to CCD. However, all CCDs are fixed to the HiRISE focal plane, the line rate stays same for every CCD. In order to retrieve exterior orientation parameters for a specific CCD image, the observation time is plugged into the SPICE kernel for interpolation. HiRISE CCDs have different observation time for each line, and as a result, different exterior orientation parameters values. However, they will all share the same exterior orientation parameters at any one moment in time. This significant characteristic makes it possible to uniformly model exterior orientation parameters that can be applied to different CCDs. Thus, images simultaneously acquired by multiple CCD arrays can be processed together under one rigorous sensor model in the bundle adjustment instead of being processed strip by strip separately.

Previous researches showed that the change in exterior orientation parameters over relatively short trajectories can be modeled using polynomials (Yoon and Shan 2005; Li et al., 2007, 2008). The pointing angles obtained from the CK data have rather coarse resolution of 35 μrad and sampling interval of 0.1 seconds, or about 1000 image lines (Kirk, et al., 2008). In practice, second-order polynomials can represent most of the movement in terms of the orbiter trajectory and the pointing direction. Using higher order polynomial functions would increase the ability to model more detailed movement. However, the movement controlled by the terms with orders higher than three have such small magnitude that it is almost negligible. Therefore, in this research, third-order polynomials are used to model the exterior orientation parameters (Li et al., 2008).

Generally, the third order polynomial model can model the satellite position very well with the magnitude of the residuals less than 0.1 mm. On the other hand, the residuals of the pointing angles are in the magnitude of ±5 μrad, sometimes exceeding more than 10 μrad, which is equivalent to about 10 pixels in the image space. This amount is certainly not negligible in high resolution image processing. It indicates that unlike the orbiter position, the image pointing parameters are not completely modeled by the polynomials. Considering the sampling interval (0.1 second) and precision (35 μrad), the residuals of ±5 μrad are considered to be sampling errors caused by lack of precision. On the other hand, jitter is high frequency random patterns that cannot be modeled by, for example, polynomials.

The causes of jitter include spacecraft vibrations associated with solar panels or a particular instrument, thermal changes and others. HiRISE stereo observations are usually obtained in high-stability mode by temporarily halting the main sources of spacecraft vibration. In this case, the effects of unexpected motions are at most 1 to 2 pixels with small oscillations of less than 1 pixel in amplitude.

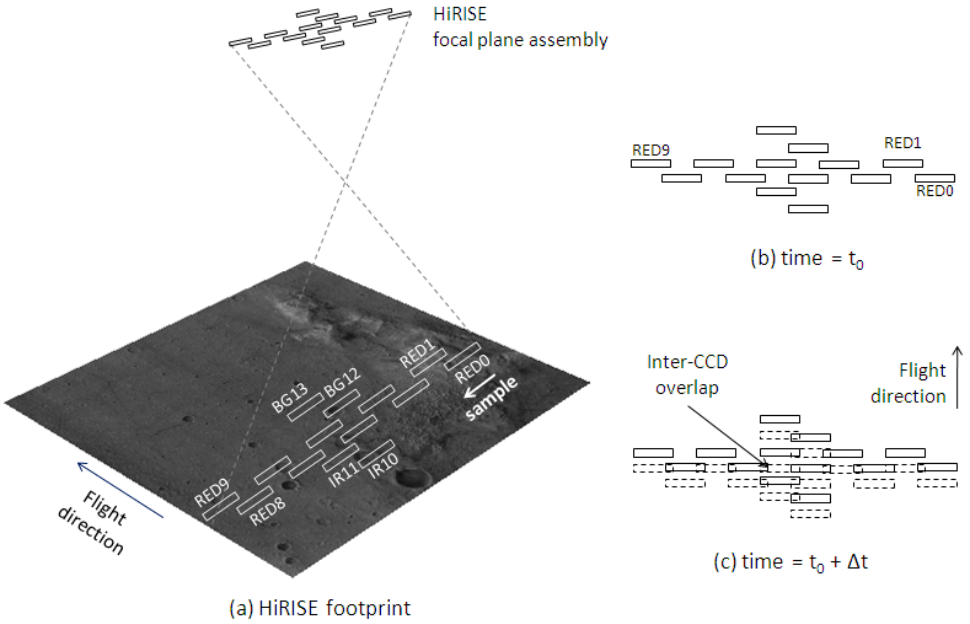

Figure 1. Illustration of jitter observation.

Not only the effect of orbital jitter needs to be evaluated for topographic mapping capability analysis of the HiRISE camera, but also it should be considered in the sensor model in order to achieve the highest mapping accuracy. Although the angular resolution and sampling interval in SPICE dataset are not precise or dense enough to fully model the jitter movement, the unique design of HiRISE CCD arrangement allows us the glimpse of its effect. Adjacent HiRISE CCDs have about 48 pixels of overlap in the across-track direction and about 7 mm of offset in the along-track direction. Figure 1 illustrates how spacecraft jitter can be observed by the inter-CCD overlap. Figure 1a shows the footprint of each CCD overlaid on a Martian terrain. Since HiRISE is a push-broom scanner, the footprints swipe through the terrain in the direction of flight. Due to the relative displacement of CCDs in the focal plane assembly, the footprint of RED1 CCD lies ahead of the footprint of RED0 CCD. This creates multiple observation of the same object with adjacent CCDs at different times. Figure 1b is the footprint at time t_0 and 1c is the footprint at time $t_0+\Delta t$, when the inter-CCD overlap of adjacent CCDs hit the same ground observed at time t_0. The typical time interval between RED CCDs are about 0.05 second, which is equivalent to about 550 lines, depending on the line rate. In the ideal case, the orbiter would move in constant speed without changing orientation angles. Then the image space coordinates of the same objects in the overlapping CCDs should maintain constant offset. However, the offsets change slightly over time or from line to line due to jitter, the irregular movement of the orbiter, Such changes in offsets cause geometric inconsistencies between CCDs in DTM generation

Bundle Adjustment of HiRISE Stereo Images

The purpose of bundle adjustment is to remove geometric inconsistencies between measurements from the stereo images. In bundle adjustment, the exterior orientation parameters are modified according to the observation equations based on the initial exterior orientation parameters and the tie points. Since no ground control points are available on Mars, additional DTM data is used as control information to achieve absolute positioning of the orbital tracks. Since HiRISE CCDs are fixed on the single focal plane assembly, a single polynomial model can applied to all the CCDs in the HiRISE frame using acquisition time as variables. In this way, bundle adjustment can be accomplished by adjusting only one set of polynomial coefficients.

The unknowns, such as exterior orientation parameters and object point coordinates, are updated iteratively by solving observation equations. In the bundle adjustment of HiRISE stereo images, there are two types of observations. The first type is the observed exterior orientation of each image line based on recorded telemetry data

from satellite tracking. The second type is the measured image coordinates of tie points on stereo images. For each image line, there are observed parameters of exterior orientation. Instead of using every image line for observation equations, only selected of image lines are used in the bundle adjustment to improve computational efficiency. Since the exterior orientation parameters are already modeled as polynomial functions, using several equally spaced lines provides enough information to control the relative variance throughout lines.

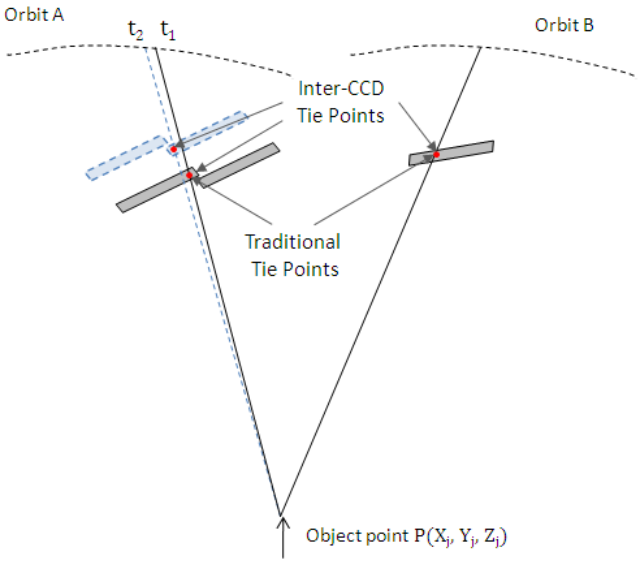

Figure 2. Traditional tie points and inter-CCD tie points.

The second type of observation equations are provided by image tie points. On the stereo images, coordinates of corresponding tie points are measured. From the measured row (line) coordinates of the tie points, time index can be obtained to derive exterior orientation parameters from the polynomial functions. Using the calibrated interior orientation and the polynomial model of exterior orientation, a rigorous geometric model is established to connect an image coordinates to the corresponding object coordinates via the collinearity equations. The ground coordinates of these image tie points are then calculated by space intersection. The observation equations are obtained by plugging in the measured image coordinates, approximate ground coordinates of the tie points and the exterior orientation parameters into the linearized form of the collinearity equations.

Tie points are selected from the matched interest points and checked for even distribution. There are two categories of tie points used for the HiRISE bundle adjustment in this research: traditional tie points and inter-CCD tie points. Traditional tie points are consisted of two corresponding matched points from stereo images. Inter-CCD tie points are traditional tie points plus additional image coordinates of the same object from another CCD of the same image. Since Inter-CCD tie points connects adjacent CCDs in a single HiRISE orbit, this particular measurement can eliminate the internal disagreement between the CCDs. Since HiRISE CCDs are arranged with a certain interval in the along-track direction, inter-CCD tie points are obtained at different times with each other. In Figure 2, one tie point on the orbit A is acquired at time t_1, while another tie point of the same object is captured on different CCD at time t_2. In fact, the inter-CCD tie points reflect the change of the orientation between the time t_1 and t_2. As discussed earlier, jitter movement is high-frequency variation of the rotation angles, causing the relative position of image coordinates between overlapping CCDs. Hence, the elimination of the disagreement between overlapping CCDs can contribute to the removal of jitter effect.

Stereo Image Processing

For automatic high-quality topographic products generation, sophisticated image matching technology is needed and it can be provided by the commercial photogrammetric suite such as BAE Systems SOCET SET ® and Leica Photogrammetry Suite. Image matching is a big topic itself and numerous researches have already been conducted (Helava, 1988; Zhang, B., and S. Miller, 1997; DeVenecia et al., 2007). For high-quality topographic product, tie point generation part could be completed using the commercial software widely used in the photogrammetric field. The limitation of using commercial software is the lack of flexibility in sensor modeling. Since the rigorous HiRISE multi-CCD sensor model is not available in commercial photogrammetric suites, the raw images from individual

CCDs need to be converted into a generic pushbroom sensor model. In this paper, a simple area-based matching method is used based on cross-correlation to generate DTM without manual editing. DTMs generated from this approach showed apparent gaps in elevation between CCDs because a generic sensor model does not solve misalignment problem.

Incorporation into MOLA Control Network

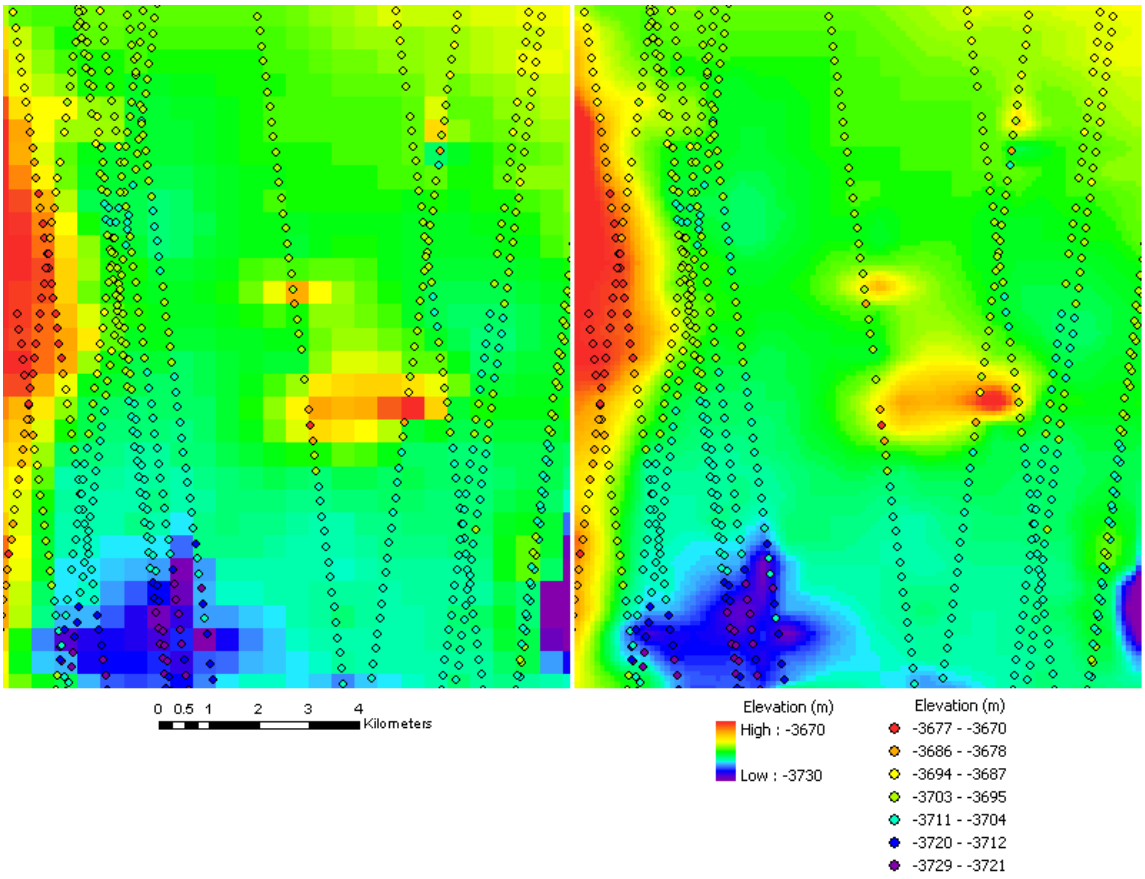

Figure 3. MOLA PEDR point data and DTM at the Spirit landing site used for HiRISE vertical control (Left) MOLA MEGDR DTM (463 m/pixel), (right) resampled MOLA DTM (100 m/pixel).

In practice, the HiRISE DTM generated by using only telemetry data may disagree with the MOLA control network by hundreds of meters. After resolving disagreement between stereo images by bundle adjustment, the MOLA DTM and profile are used as elevation control information for approximation of the absolute positioning. Since there is no ground control point available on Mars, it is not feasible to directly connect image points with ground points. In this research, the terrain generated by HiRISE stereo was compared and matched to the MOLA DTM before using MOLA points as vertical control. This correlation-based matching technique treats DTMs as images and matches DTMs according to image correlation. The description about the terrain matching can be found in Hwangbo et al. (2009).

The most detailed MOLA DTM product for non-polar region is MEGDR with resolution of 128 pixels per degree, which is equivalent to about 463 meters of grid size in equirectangular projection. On average, the horizontal accuracy of MEGDR product is expected to be about 200 m and the vertical accuracy is on the order of 10 m (Gwinner, 2009). The horizontal resolution of the MOLA DTM is significantly lower than that of HiRISE imagery (25 cm/pixel). Since the purpose of the terrain matching is to obtain approximated absolute position before precise adjustment of exterior orientation parameters, the common grid size for the terrain matching is set as 100 m. MEGDR product is resampled into 100-m grid by bilinear interpolation. HiRISE DTM with the same grid size is generated by Kriging method using 10-pixel grid points.

From the terrain matching, the amount of shift in object space is obtained based on the initial object space coordinates of the HiRISE DTM and the MOLA DTM. As can be seen from Figure 3, there are areas where the MEGDR DTM is interpolated due to limited coverage of MOLA tracks, especially the Columbia Hills. Therefore, the 3-D coordinates of MOLA PEDR points are matched afterward to conduct tighter absolute positioning. The reason of conducting DTM-based terrain matching prior is to obtain approximate horizontal position first to reduce the amount of horizontal shift during matching the terrain against the PEDR points. In the example above, the MOLA points are about 300 m apart from each other. In the terrain match, the position of HiRISE DTM is adjusted up to a few kilometers. In the MOLA point vertical control, the adjustment of horizontal position is confined to 500 m, given that the resolution of MEGDR DTM is 463 m.

In this research, bundle adjustment of exterior orientation parameters was conducted separately from absolute positioning by MOLA control networks. First, discrepancies between HiRISE stereo images and CCDs are resolved by bundle adjustment with weighting parameters based on a priori accuracy of the position and the orientation. Afterward, the DTM generated after bundle adjustment is matched with the MOLA DTM and points to determine horizontal and vertical shifts of the HiRISE stereo image network. The reason for using such strategy for orbital image network generation on Mars is twofold: precision and simplicity. Despite considerable shift from the MOLA DTM, the precision of MRO exterior orientation parameters is far better than any dataset used to generate the Mars control network. Increasing the variances for weight parameters means loose weighting, which allows more adjustment of the observed values. However, loose weighting could also lead to possible loss of precision in the original MRO exterior orientation dataset. However, it is contradictory to the known a priori variances of MRO exterior orientation parameters. By using the known variances for weighting in the bundle adjustment system, the precision of the exterior orientation parameters is preserved.

EXPERIMENTAL RESULTS AND DISCUSSION

Topographic mapping products are generated from the stereo pair of HiRISE images PSP_001513_1655 and PSP_001777_1650, which cover the Columbia Hills area of the Spirit rover landing site. The coverage of the stereo images includes the areas where Spirit rover landed and had explored for the past four years. The PSP_001513_1655 image was obtained on November 22, 2006. It is centered at 14.6 °S latitude, 175.5°E longitude. It has 27.1 cm/pixel resolution and 80,000 rows. The PSP_001777_1650 image was taken on December 12, 2006. It has a resolution of 26.3 cm/pixel and 40,000 rows. Its extent, about 10.5 km × 5.5 km on the ground, is entirely covered by PSP_001513_1655. The two images have a convergence angle of 19.8 degrees.

In this research, the bundle adjustment is conducted on the HiRISE stereo images. Each HiRISE image is consisted of ten red band CCD strips. For the best performance of bundle adjustment, evenly distributed tie points are needed. Both traditional and inter-CCD tie points are automatically selected from the matched interest points of the stereo images. For bundle adjustment, 270 traditional image tie points are selected. From matched interest points in the overlapping area between adjacent CCDs of PSP_001777_1650 image, 80 inter-CCD tie points are selected. Likewise, 80 inter-CCD tie points are chosen from the overlap area of PSP_001513_1655 image. Due to severe noise present in PSP_001777_1650 CCD9 image, tie points in the CCD9 are not used in the bundle adjustment process. Among the nine overlap areas between the ten CCDs, the inter-CCD tie points from the overlap between CCD8 and CCD9 was also excluded.

The polynomial coefficients of the exterior orientation parameters are adjusted based on the measured image coordinates of the tie points. Since there is no absolute ground truth is available on the Martian surface, ground control points could not be used to evaluate the performance of bundle adjustment. Instead, 430 check points, which were not used in the bundle adjustment process, were selected from matched interest points. The check points are consisted of 270 traditional tie points, 80 inter-CCD tie points for PSP_001513_1655 and PSP_001777_1650, respectively. The ground coordinates of the check points are obtained by space intersection and back projected on each stereo image. The differences between the back-projected image coordinates and the original measurements are compared to evaluate the performance of the bundle adjustment.

Observations in the bundle adjustment, exterior orientation parameters and the measured image coordinates, have their own units and scales. Therefore, different weights are assigned to each observation equation to properly account for the magnitude of adjustment. The weights are decided according to a priori variances. If unit weight is chosen as 1, the weight p is assigned by dividing the observed parameter by it's *a priori* variance σ^2. For bundle adjustment of HiRISE images, *a priori* variance of tie point coordinates is set as half a pixel, or 6 μm. The estimated uncertainty of the MRO trajectory is about 5 m for orbits at the beginning of the mission, and within about 1 m for

later orbits. As for the rotation angles, the known precision of the pointing data is 0.035 mRad and systematic errors are considered to be no greater than 0.3 mRad (Kirk et al., 2008).

The implementation of bundle adjustment is an iterative process of modifying the polynomial coefficients of the exterior orientation parameters by solving the linearized observation equations. In this research, eight cases of bundle adjustment are tested using different weighting parameters, tie points and control data. Table 1 shows the statistical results of the back projection residuals from three types of check points. In the table, 'A' stands for traditional tie points, 'B' is PSP_001513_1655 inter-CCD tie points, and 'C' is inter-CCD tie points of image PSP_001777_1650. Before bundle adjustment, the mean magnitudes of back projection residuals were over three pixels and the standard deviations were over two pixels. In other words, there is no sign of major disagreement between the original exterior orientation parameters of the stereo images.

Table 1. Statistics of back projection residuals of check points (unit in pixels)

	Variances used for weight			Magnitudes of back projection residuals mean (standard deviation)			Maximum differences in exterior orientation parameters after bundle adjustment	
Bundle adjustment method	σ_X, σ_Y, σ_Z (m)	σ_ω, σ_φ, σ_κ (mRad)	σ_x, σ_y (pixel)	A (pixel)	B (pixel)	C (pixel)	σ_X, σ_Y, σ_Z (m)	σ_ω, σ_φ, σ_κ (mRad)
-	-	-	-	3.73 (2.86)	3.37 (2.32)	4.77 (2.93)	-	-
1	1	0.3	0.5	0.17 (0.12)	1.39 (0.49)	0.97 (0.35)	0.03	0.13
2a	1	0.05	0.5	0.17 (0.12)	0.52 (0.24)	0.55 (0.25)	0.87	0.16
2b	1	0.1	0.5	0.17 (0.12)	0.52 (0.23)	0.51 (0.24)	0.26	0.20
2c	1	0.3	0.5	0.17 (0.12)	0.52 (0.23)	0.51 (0.21)	0.04	0.31
2d	5	0.3	0.5	0.17 (0.12)	0.52 (0.23)	0.51 (0.21)	0.10	0.30
2e	100	0.3	0.5	0.17 (0.12)	0.51 (0.23)	0.48 (0.21)	113	0.24
2f	100	8.73	0.5	0.16 (0.11)	0.50 (0.25)	0.45 (0.22)	80	5.30
3	100	0.3	0.5	0.34 (0.26)	1.26 (0.53)	1.04 (0.48)	1225	6.19

Eight methods of bundle adjustment were tested using different types of tie points and weighting parameters. Method 1 used only traditional tie points and the variances for weighting parameters are set as 1 m for position, 0.3 mRad for orientation, 0.5 pixel for image coordinates. In bundle adjustment system, the ratios between weight parameters rather than their absolute values affect results. Therefore, the variance for image coordinates is fixed to 0.5 pixel in this experiment. After bundle adjustment, the mean magnitude of back projection residuals between stereos (A) was significantly reduced to 0.17 pixel, but the mean residuals between inter-CCD overlap were not as drastically reduced. Type B residual in PSP_001513_1655 was still 1.39 pixel, and type C residual was 0.97 pixel. This means that traditional tie points alone are not enough to compensate for the disagreement between overlapping CCDs.

Method 2a through 2f use the same observation equations from both traditional and inter-CCD tie points, although the variances of satellite position and rotation angles were set differently. The tightest weighting is applied in method 2a, while the loosest in method 2f. However, the back projection residual, which indicates the effectiveness of bundle adjustment, remain consistent regardless of the weighting. After bundle adjustment method 2a is implemented, the mean magnitude of inter-CCD back projection residuals was 0.52 pixel for type B and 0.55 pixel for type C. Since the image coordinates precision of tie points is about 0.5 pixel, it is reasonable to say that the disagreement between CCDs are resolved. As variances for rotation angles are increased to 0.1 mRad (method 2b) and 0.3 mRad (method 2c), the residuals on inter-CCD tie points are slightly improved. When method 2c is compared to method 2b, looser weighting for position did not further reduce errors. In this case, using the known accuracy of telemetry position for weighting parameters was sufficient for resolving displacement between stereo. Method 2d and 2e applied much larger position variances (100 m) used by USGS, and 8.73 mRad of pointing angle variance is equivalent to 0.5 degree specifically used for the Spirit landing site stereo. Compared to method 2c, looser weighting in position applied to method 2d brought the back projection residual down by 0.01 pixel for type B and 0.03 pixel for type C check points. However, method 2f resulted in smaller mean magnitudes of residuals, but the standard deviation of the inter-CCD check points actually went up. Method 3 uses similar strategy as USGS, allowing free shift and drift of exterior orientation parameters and incorporating MOLA elevation profile. Since MOLA control network points are not identifiable in HiRISE imagery to only the residuals in elevation were

included as input of observation equation in the bundle adjustment system. The back projection residuals are about two times bigger than the residuals from the proposed method.

Although the statistics of the back projection residuals look similar for methods 2a through 2f in Table 1, the changes in exterior orientation parameters vary significantly depending on the weighting parameters. In general, the variances for weighting determined the magnitudes of the changes in exterior orientation parameters. However, The pattern of the change is not exactly predictable. Compared to method 2a, method 2b has twice bigger variance for rotation angles and the same variance for position. However, the rotation angles are almost same and the differences in position increased about three times. Method 2d has five times bigger variances for position, its position change went up 25 times bigger than method 2c, while the rotation angles were about the same. Although bigger variances generally mean more change in exterior orientation parameters, the amount of change is not proportional to the variances. Increasing variance of one parameter impacts other parameters as well. The bundle adjustment results in method 2e and method 2f exceeds the expected amount of changes in exterior orientation parameters. The small back projection residuals before bundle adjustment demonstrate that the original telemetry data is in good shape and the stereo images align relatively well with each other. Method 2a through method 2f reduced the residuals to the very similar level, the differences being less than 0.1 pixel. Increasing the variances for weighting does not guarantee produce better results, but could cause unnecessary changes in the exterior orientation parameters instead. Since the disagreement between stereos and CCDs could be resolved even using tightest weighting, it is reasonable to use variances that are consistent with the known accuracies of the parameters. In HiRISE telemetry data, the uncertainties are 1 m for position, and 0.3 mRad (about 0.017 degree) for rotation angels. Therefore, bundle adjustment was conducted using method 2c in this paper. Since the MOLA profile does not provide exact ground control points, the incorporation of MOLA control using loose weighting parameters (method 3) actually produced unnecessary adjustment and worse bundle adjustment result for the HiRISE stereo. Therefore, the bundle adjustment between stereo images and CCDs was conducted separately from the absolute positioning based on MOLA control networks.

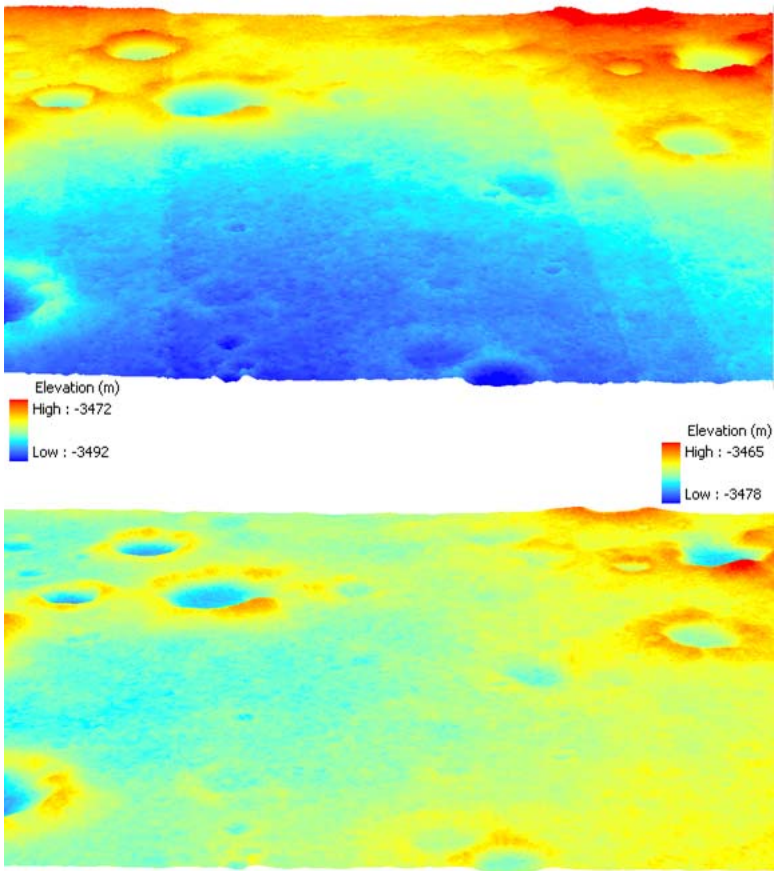

Figure 4. 3-D surface map of HiRISE DTM with 3x vertically exaggeration. Surface map generated from exterior orientation parameters after method 1 bundle adjustment (top), and method 4 bundle adjustment (bottom).

After method 2c bundle adjustments, the differences of the perspective center positions are smaller than 1 meter and the changes of pointing angles are less than 0.3 mRad. The significantly reduced error vectors demonstrate that the inconsistencies between the stereo pairs are successfully removed by the bundle adjustment proposed in this research and that the incorporation of inter-CCD tie points renders better results in the rigorous sensor model. The bundle adjustment results can be evaluated in the object space. As shown in table 1, the ground coordinates calculated using the original telemetry exterior orientation parameters have inconsistencies between the points from overlapping CCDs. Comparison of the ground coordinates between two inter-CCD tie points on one stereo intersected with the corresponding image point on the other stereo can give us information about such discrepancies. Figure 4 shows two DTM surface maps using exterior orientation parameters from method 1 (with traditional tie points only) and method 2c (both traditional and inter-CCD tie points) bundle adjustment. The first one was generated using refined exterior orientation based on bundle adjustment using only traditional tie points and the second one used exterior orientation adjusted based on both traditional and inter-CCD points. The first surface map has strong artifacts which were caused by geometric inconsistencies between overlapping CCDs. The second surface map shows a seamless homogenous surface even though it is physically generated by different CCD strips. The inconsistencies were not removed by bundle adjustment until inter-CCD tie points were incorporated. The effectiveness of the proposed bundle adjustment with inter-CCD tie points is visually confirmed in the surface map comparison. The average difference of ground coordinates between CCDs was about 1 meter after method 1 bundle adjustment. Using inter-CCD tie points in the method 4 bundle adjustment system, the average difference is reduced to 0.3 meter. The inconsistencies between the overlapping CCDs are successfully removed by incorporating inter-CCD tie points in bundle adjustment.

Absolute Positioning using MOLA Control Network

After removing inconsistencies of exterior orientation parameters between the stereo images and between the CCDs, absolute positioning of HiRISE image is conducted using MOLA control network. The HiRISE DTM is first matched to MEGDR DTM, which was resampled to 100-m resolution grid. During the terrain match, the search area was set to 5 kilometers. Based on the initial positioning, the MOLA points from PEDR dataset (shown as regularly spaced circles in Figure 2) were further matched with HiRISE DTM. The extent of the second search area is set to 500 m. After terrain match against the 3-D coordinates from PEDR points, the HiRISE DTM shifted from its original position by 200 m to the west, 100 m to the north, and -232.45 m vertically (FIgure 5). In this test dataset, the horizontal shift of HiRISE DTM is less than 230 m, which is well below the search area for the second terrain match. Due to the irregular coverage of PEDR dataset terrain match is conducted twice first with MEGDR DTM and then with PEDR points. MEGDR DTM is interpolated elevation data, whereas PEDR data is the actual measurement of the Martian terrain. Therefore, broader terrain matching is conducted with MEGDR DTM to conduct approximate positioning and later PEDR points are matched for precise absolute positioning.

The Spirit rover landing position, which is also the origin of Local Coordinate System, is centered at 175.47848 º in longitude and −14.571892 º in latitude (Golombek and Parker, 2004). The location was obtained based on comprehensive rover localization and photogrammetric analysis of various orbital dataset after the landing. In this research, the knowledge of the rover's landing position is used to validate the absolute positioning result. The origin of Spirit rover traverse can be identified on the HiRISE image since the debris of the landing unit is left on the ground, which is the bright object inside the green circle in Figure 5. The known Spirit rover landing position is displayed as yellow circle in the figure. The Spirit rover landing position in the HiRISE topographic products generated using the original exterior orientation parameters before bundle adjustment is displayed as black circle and about 200 m apart from the known position. After absolute positioning using the MOLA control, the displacement is reduced to 65 m. In the USGS orthophoto (Kirk et al. 2008), the difference of position is about 270 m. Considering that the horizontal accuracy of the MOLA dataset is about 100 m (Smith et al., 2001), the absolute positioning using MOLA DTM and points were successful within the accuracy level of the control network.

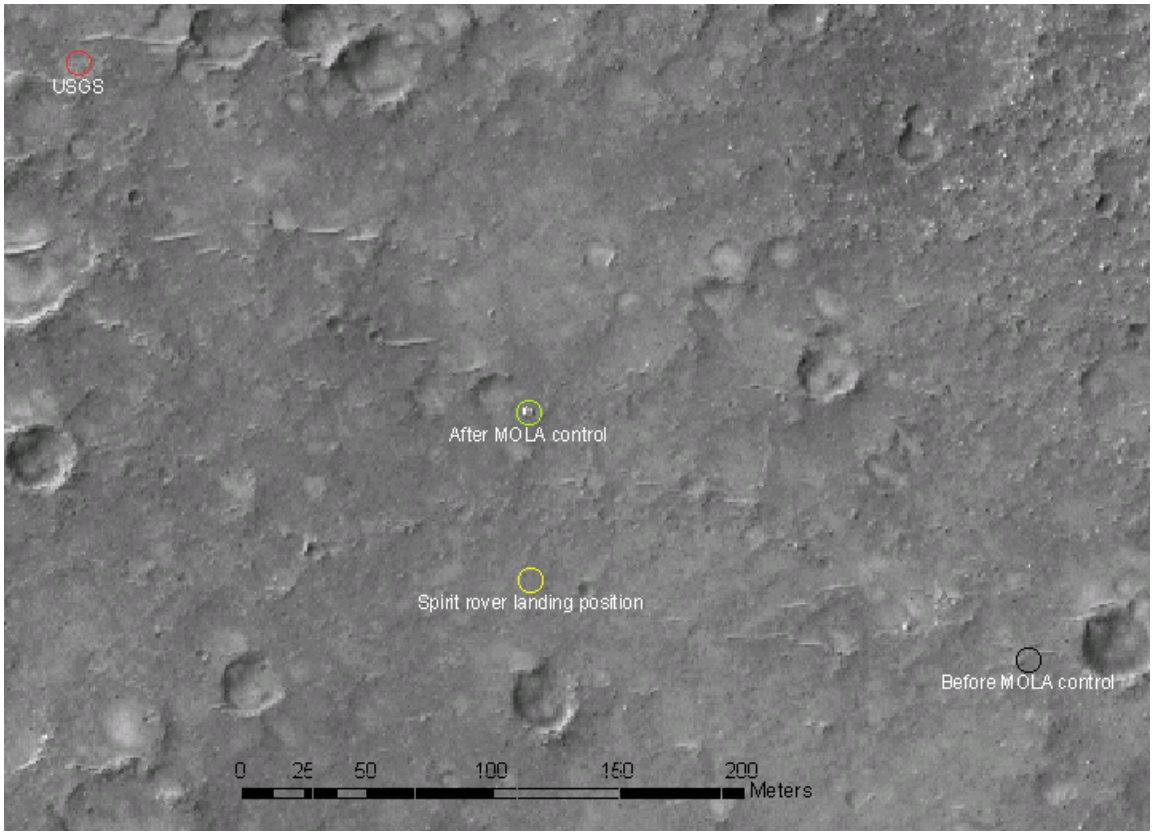

Figure 5. HiRISE Orthophoto generated after absolute positioning using MOLA control compared with the known Spirit rover landing position.

CONCLUSION

For construction of orbital image networks, bundle adjustment system based on tie points is developed to resolve misalignment of exterior orientation parameters between stereo images and CCDs. Bundle adjustment based on polynomial function model of exterior orientation parameters was conducted. In addition to traditional tie points, inter-CCD tie points between multiple CCDs in a single orbit are used to minimize geometric inconsistencies between CCDs caused by jitter. The proposed bundle adjustment method based on third-order polynomials reduced mean back projection error of traditional tie points from over 3 pixels to less than 0.2 pixel for the test dataset covering Spirit rover landing site. The back projection residual between inter-CCD tie points were also reduced to about half a pixel. Bundle adjustment without using inter-CCD tie points only reduced the inter-CCD residual to about one pixel. To achieve consistent orbital image network construction without ground-control points, HiRISE DTM is matched with MOLA MEDGR DTM and PEDR profile after bundle adjustment. Based on the terrain matching results, the position of HiRISE orbital image network is shifted to achieve absolute geopositioining based on MOLA global Mars terrain model. The absolute positioning result is compared with the Spirit rover landing position visible on the HiRISE image. The displacement is reduced from about 200 m to 65 m, which is successful given the MOLA horizontal accuracy of 100 m.

Although the proposed methods are successfully implemented in the test site, there are some issues that need to be improved. Although the proposed bundle adjustment system using inter-CCD tie points, the back projection residual between overlapping CCDs (about 0.5 pixel) were still three times bigger than the residual between traditional tie points (about 0.17 pixel). In this research, one polynomial function describing the exterior orientation parameters is applied to all the CCDs. Applying more flexibility between the CCDs could further reduce the inter-CCD misalignment and resolve jitter.

ACKNOWLEDGEMENTS

Funding for this research by the NASA Mars Applied Information Systems Research Program is acknowledged.

REFERENCES

Acton, C. H., 1999. SPICE products available to the planetary science community, Lunar Planet. Sci., XXX, abstract 1233.

Devencia, K., S. Walker and B. Zhang, 2007. New Approaches to Generating and Processing High Resolution Elevation Data with Imagery. Photogrammetric Week, 17 (5): 1442-1448.

Golombek, M. and T. Parker, 2004. Lander localization, *MER ProjectMemorandum* (one for Spirit, one for Opportunity), JPL/NASA.

Gwinner, K., F. Scholten, M. Spiegel, R. Schmidt, B. Giese, J. Oberst, C. Heipke, R. Jaumann and G. Neukumm 2009. Derivation and Validation of High-Resolution Digital Terrain Models from Mars Express HRSC-Data, Photogrammetric Engineering & Remote Sensing, 75(9): 1127–1142.

Heleva, U.V, 1988. Object space least square correlation, Photogrammetric Engineering & Remote Sensing, 54(6): 711-714.

Hwangbo, J., K. Di and R. Li, 2009. Integration of Orbital and Ground Image Networks for the Automation of Rover Localization. ASPRS 2009 Annual Conference, Mar, 9-13, 2009, Baltimore, MD.

Kirk R.L., E. Howington-Kraus, M.R. Rosiek, J.A. Anderson, B.A. Archinal, K.J. Becker, D.A. Cook, D.M. Galuszka, P.E. Geissler, T.M. Hare, I.M. Holmberg, L.P. Keszthelyi, B.L. Redding, W.A. Delamere, D. Gallagher, J.D. Chapel, E.M. Eliason, R. King, and A.S. McEwen, 2008. Ultrahigh resolution topographic mapping of Mars with MRO HiRISE stereo images: Meter-scale slopes of candidate Phoenix landing sites, *J. Geophys. Re*s., *113*, E00A24, doi:10.1029/2007JE003000.

Li, R., K. Di, L.H. Matthies, R.E. Arvidson, W.M. Folkner, and B.A. Archinal, 2004. Rover localization and landing site mapping technology for 2003 Mars Exploration Rover mission. *Photogrammetric Engineering & Remote Sensing*, 70(1): 77-90.

Li, R., S.W. Squyres, R.E. Arvidson, B.A. Archinal, J. Bell, Y. Cheng, L. Crumpler, D.J. Des Marals, K. Di, T.A. Ely, M. Golombek, E. Graat, J. Grant, J. Gulnn, A. Johnson, R. Greeley, R.L. Kirk, M. Maimone, L.H. Matthies, M. Malin, T. Parker, M. Sims, L.A. Soderblom, S. Thompson, J. Wang, P. Whelley and F. Xu, 2005. Initial results of rover localization and topographic mapping for the 2003 Mars Exploration Rover mission. *Photogrammetric Engineering & Remote Sensing*, 71(10): 1129–1142.

Li, R., R.E. Arvidson, K. Di, M, Golombek, J. Guinn, A. Johnson, M. Maimone, L.H. Matthies, M. Malin, T. Parker, S.W. Squyres and W.A. Watters, 2007. Opportunity rover localization and topographic mapping at the landing site of Meridiani Planum, Mars. Mars, J. Geophys. Res., 112, E02S90, doi:10.1029/2006JE002776.

Li, R., J. Hwangbo, Y. Chen, and K. Di, 2008. Rigorous Photogrammetric Processing of HiRISE Stereo Images for Mars Topographic Mapping. *XXI ISPRS Congress*, Beijing, China, July 2008.

McEwen, A.S., E. M. Eliason, J.W. Bergstrom, N. T. Bridges, C. J. Hansen, W. A. Delamere, J. A. Grant, V. C. Gulick, K. E. Herkenhoff, L. Keszthelyi, R. L. Kirk, M.T. Mellon, S. W. Squyres, N. Thomas, and C. M. Weitz, 2007. Mars Reconnaissance Orbiter's High Resolution Imaging Science Experiment (HiRISE), *J. Geophys. Res.*, *112*, E05S02, doi:10.1029/2005JE002605.

Shan, J., J-S.Yoon, S. Lee, R. Kirk, G. Neumann, and C. Acton, 2005. Photogrammetric Analysis of the Mars Global Surveyor Mapping Data, *Photogrammetric Engineering &Remote Sensing*, 71(1): 97-108.

Smith, D. E., M. T. Zuber, H. V. Frey, J. B. Garvin, J. W. Head, D. O. Muhleman, G. H. Pettengill, R. J. Phillips, S. c. Solomon, H. J. Zwally, W. B. Banerdt, T. C. Duxbury, M. P. Golombek, F. G. Lemoine, G. A. Neumann, D. D. Rowlands, O. Aharonson, P. G. Ford, A. B. Ivanov, C. L. Johnson, P. J. McGovern, J. B. Abshire, R. S. Afzal and X. Sun, 2001. Mars Orbiter Laser Altimeter: Experiment summary after the first year of global mapping of Mars, J. Geophys. Res., 108(E12), doi: 10.1029/2000JE001364, pp. 23689-23722.

Yoon, J. and J. Shan, 2005. Combined adjustment of MOC stereo imagery and MOLA altimetry data, Photogrammetric Engineering and Remote Sensing, 71(10): 1179–1186.

Zhang, B. and S. Millter, 1997. Adaptive Automatic terrain Extraction. McKeown, D.M., McGlone, J.C., Jamet, O. (eds.), Proceedings of SPIE, Vol. 3072, Integrating Photogrammetric Techniques with Scene Analysis and Machine Vision III, pp. 27-36.